

# Design of a Family of Mars Chemical Transportation Elements

Douglas J. Trent<sup>1</sup> and Stephen J. Edwards<sup>2</sup> and Michael B. Chappell<sup>3</sup>  
*NASA Marshall Space Flight Center, Huntsville, AL, 35812, U.S.A.*

**NASA’s Mars Architecture Team (MAT) has recently developed a collection of concepts to assess the capabilities and constraints presented by architectures incorporating large-scale Mars In-Situ Resource Utilization (ISRU) propellant production. The focus of this manuscript is on the concept design of chemical propellant-based transportation systems including a dual role lander/ascent vehicle and an in-space transporter. Mission performance analyses performed during a recent design analysis cycle derived the 300,000 kg propellant production capacity utilized for preliminary concept designs of enabling surface ISRU systems, power systems, fluid handling systems, and their concept of operation, detailed in companion papers.**

## I. Nomenclature

ACS	= Attitude Control System
EUS	= Exploration Upper Stage
ISRU	= In-Situ Resource Utilization
LDHEO	= Lunar Distant High Earth Orbit
LPS	= Landing Propulsion System
MALV	= Mars Ascent/Lander Vehicle
MACHETE	= Mars Chemical Transportation Elements
MIST	= Mars In-Space Transport
MPS	= Main Propulsion System
NRHO	= Near Rectilinear Halo Orbit
POST2	= Program to Optimize Simulated Trajectories II
RDRE	= Rotating Detonation Rocket Engine
TMI	= Trans Mars Injection
TPS	= Thermal Protection System

## II. Introduction

Human Mars mission planning is an ongoing and evolving activity, dating back to the first integrated Mars architecture concept put forward by von Braun in 1953 [1]. The continuous study, reformulation, and refinement of Mars architectures and system concepts is necessary to incorporate updated mission objectives [2], technology advancements, and growth in the body of knowledge regarding human factors and the various environments encountered in human space flight. Architecture concepts of note in recent years include NASA’s Design Reference Architecture 5.0 in 2009 [3], the Evolvable Mars Campaign in 2016 [4], and a minimum surface infrastructure architecture in 2020. [5], [6]

As part of the formulation and evaluation of these architecture alternatives, numerous studies have been performed on concepts for Mars Entry, Descent, Landing, and Ascent (EDLA) systems. [7]-[15] The multiple trades on mission concepts and concept designs performed have focused on EDLA concepts where the “EDL” and “A” functions are split between distinct elements. However, during this timeframe there have also been a handful of architecture concepts proposed that employ a single common element to carry out the full EDLA mission. [16]-[18] In-situ resource utilization (ISRU) for propellant production, already a technology of potential benefit to any human Mars architecture,

---

<sup>1</sup> Technical Advisor, Advanced Concepts Office, NASA/MSFC ED04, AIAA Senior Member.

<sup>2</sup> Mission Architect, Advanced Concepts Office, NASA/MSFC ED04, AIAA Member.

<sup>3</sup> Engineer, NASA/MSFC ST24.

factors heavily in the paradigm espoused by architectures that employ these large single-stage EDLA elements. For this reason, evaluating these architectures is not as simple as sizing transportation systems and solving the mission performance; requisite surface systems and concepts of operation must also be identified and characterized.

In continuing to consider the many formulations available for the future human exploration of Mars, NASA's Mars Architecture Team (MAT) has recently developed a collection of concepts to assess the capabilities and constraints presented by architectures incorporating Mars ISRU for large-scale propellant production to supply large single-stage EDLA elements. This paper focuses on the transportation system for such architectures, but two companion papers address the surface systems and conops required to enable an integrated architecture solution. [19], [20] The primary objective of this work is to help NASA better understand emerging Mars architecture trade spaces in support of ongoing agency efforts, including the NASA Architecture Definition Document. [21], [22]

### III. Transportation System Overview

Combining all the functions for EDLA into a single transportation element naturally leads to a compromise design. Though not a standard decomposition, and not to be strictly interpreted, it is helpful to think of "E" (entry) as involving aerothermodynamic functions, "D" (descent) as involving propulsive (retropropulsion) functions, "L" (landing) as involving terrain sensing/navigation and surface contact functions, and "A" (ascent) primarily propulsive functions. When these functions are divided among more than one element, there is an opportunity for system specialization and optimization that is lost with a single element that must encompass them all. The single element will end up larger, heavier, and more complex than the multi-element options; however, in exchange, the single element option presents the value proposition of reducing the number of unique element developments and introducing greater potential for reuse.

The implications of a large chemical EDLA element reach beyond the transportation system. To capitalize on the reusability potential of these concepts requires Mars surface architecture features previously not studied in depth, including large scale surface ISRU, surface transfer of fluids, cryogenic fluid liquefaction and storage, and power systems to support such operations. These implications are explored in the [19] and [20] companion papers; this paper

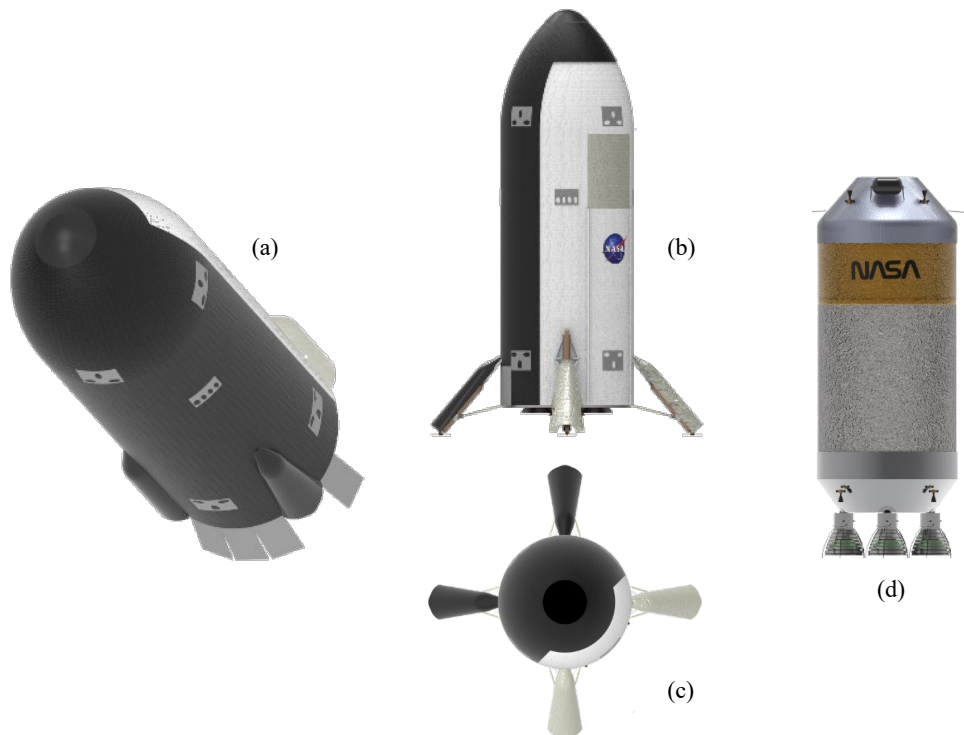


**Figure 1** MACHETE vehicles (a) MALV in entry configuration, (b) MALV in landed configuration side view, (c) MALV in landed configuration top view, and (d) MIST

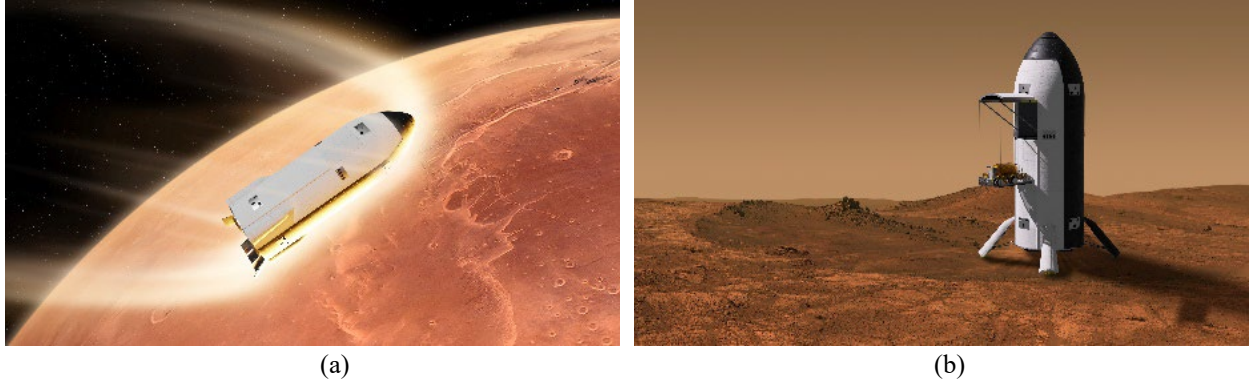


**Figure 2 Concept images of the MALV during different mission phases: (a) Mars Atmospheric Entry, and (b) Offloading Payload on the Mars Surface**

lays out the conceptual design for a family of chemical propulsion-based Mars transportation vehicles, collectively called the Mars Chemical Transportation Elements (MACHETE).

MACHETE consists of two primary configurations: the Mars Ascent/Lander Vehicle (MALV), and the Mars In-Space Transport (MIST). Figure 1 provides configuration views of the MALV and the MIST, and Figure 2 depicts artist concept images of the MALV during atmospheric entry and when offloading payload on the Mars surface. Conceptually, the MIST is a stripped-down version of the MALV, not requiring the subsystems responsible for performing the EDL functions. However, the MIST design extends the propellant tanks to make full use of the volume reserved for cargo in the MALV. Though the MACHETE family can provide full end-to-end Mars transportation, the MALV or MIST concepts can also be utilized in other transportation architectures that may employ alternative landers, ascent vehicles, or in-space transportation systems.

#### **A. Mars Ascent/Lander Vehicle (MALV) Summary**

The MALV concept is nominally designed to deliver at least 75,000 kg of payload to the surface of Mars in a single landing. This target was identified as a lower bound of landed payload mass required to support initial human missions to Mars under specific assumptions [6]. An alternate “stretched” version of the MALV concept is also under design, with the goal of enabling up to 150,000 kg of landed payload to the surface of Mars. This payload target for the stretched MALV was selected to enable delivery of all required surface systems in a single landing to simplify the overall transportation architecture.

A high-level summary of the MALV crew configuration concept is depicted in Figure 3. Detailed descriptions of each of the primary subsystems are provided in Section IV. The MALV is 8.4 meters in diameter and stands 27 meters tall. Starting from the top, the vehicle has a forward docking port to allow for crew ingress/egress with other orbital assets, such as the Mars Transit Habitat. The docking port conforms to the NASA Docking System Block 2 interface definition, which is a draft update to the interface definitions of the Block 1 standard [23]. The crew configuration of the vehicle has an integrated crew compartment designed for short term crew habitation. For a dedicated cargo MALV, the crew compartment and associated subsystems can be removed to allow for additional payload support. Below the crew cabin is the primary payloads bay, which has an integrated lift system to support payload deployment to the surface. Continuing down the vehicle, the main and secondary (header) propellant tanks are below the payload bay, followed by the main propulsion section at the bottom. The MALV also contains two other integrated propulsion systems, the landing propulsion system, and an attitude control system. The vehicle has four large landing legs to support stable touchdown on Mars, as well as deployable aft body flaps to support aerodynamic flight. The MALV has an integrated thermal protection and management system, which can support long term cryogenic fluid storage during Mars surface refueling, while also being able to withstand the extreme environment of Mars atmospheric entry. Note, there are no power systems shown. Initial concepts utilized oxygen-methane fuel cells for power generation during all phases of flight. However, subsequent analysis has considered solar-based power for long-duration in-space operations to minimize propellant consumption by fuel cells.

The stretched MALV has the same general layout and design, with the exception that the payload bay and propellant tanks are elongated to support increased payload volume and mass delivery capability. Other notable changes include increased propulsion system thrust to accommodate increased inert masses, as well as additional structural mass to support the increased loads as a result.

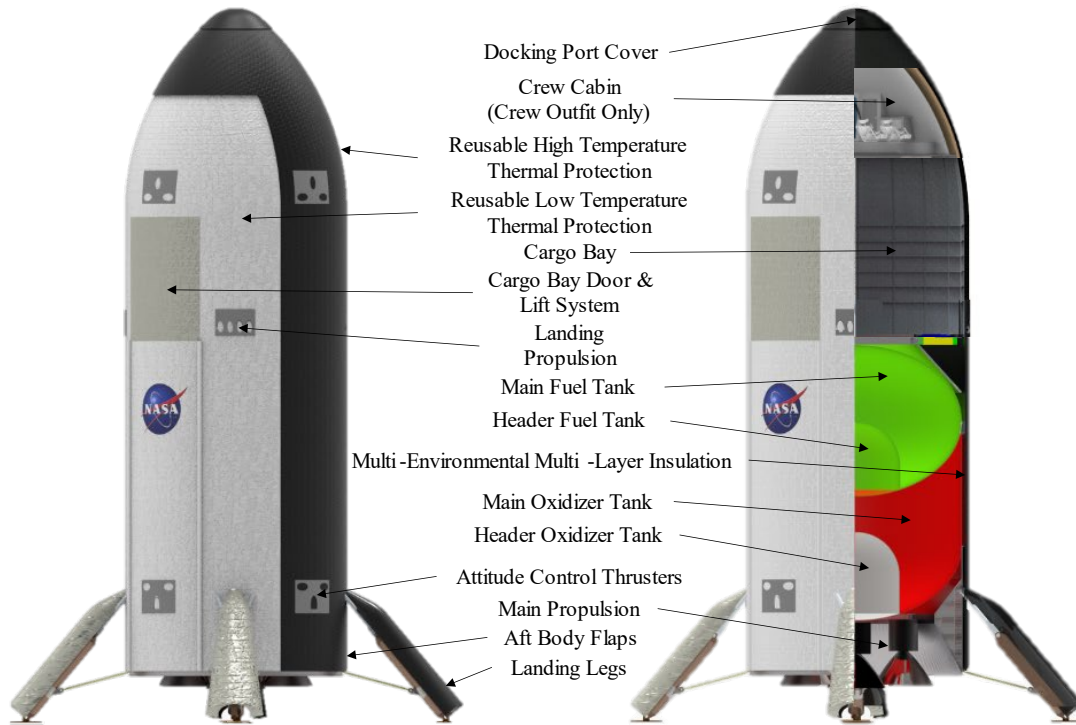


**Figure 3 MALV Crew Configuration Overview.**

### **B. Mars In-Space Transport (MIST) Summary**

The MIST system architecture is essentially equivalent to a MALV with several subsystems not necessary for a dedicated in-space transport removed. The subsystems removed include payload integration and surface offloading subsystems, thermal protection systems for atmospheric entry, aerodynamic surfaces, propulsion system header tanks and landing engines, avionics subsystems associated with terrain sensing and obstacle avoidance, and landing legs. The implementation currently being studied also removes the MALV's integrated crew habitat, assuming that in-space habitation is provided by a separate Mars Transit Habitat. This latter choice was made in the initial population of the MACHETE family to allow for more straight-forward comparisons across alternative transportation architectures; however, it remains in the trade space to consider MIST configurations which have integrated in-space habitation capability. The same major outer mold line (OML) dimensions are maintained, but the propellant tanks are stretched to take up the MALV's cargo bay and utilize the full volume available within the OML envelope.

The one major break in commonality between the MIST and the MALV system architectures is in the power system. Whereas the MALV employs a fuel-cell based power generation system utilizing the main propellants as reactants, the MIST design incorporates a solar power system. This was found to reduce propellant requirements during its much longer mission duration; interestingly, the reverse is true for the MALV, where the fuel-cell power system provides the lower propellant load requirement. Further descriptions of each of the primary subsystems are provided in Section IV.

### **C. MACHETE Campaign Concept**

The MACHETE concept family is designed to provide end-to-end in-space and Mars EDLA transportation functions for a human Mars architecture. Figure 4 depicts a notional campaign of landings in support of an initial human Mars mission. In this implementation, the architecture is executed over two Earth-Mars transit opportunities in 2037 and 2039. The 2037 opportunity is utilized to deliver cargo payloads required to support the human surface mission, and the 2039 opportunity is utilized to deliver the crew lander as well as for crew to transit to Mars. A long-held ground rule reducing loss of crew risks in NASA human Mars mission planning is that the crew's Mars ascent vehicle should be fully-fueled and ready to launch before the crew descends to the surface. For the MACHETE-based campaign concept this means that although the MALV is designed to perform the full EDLA mission, the same MALV cannot be used for both EDL and A by the same crew. The crew ascent MALV used for must be pre-deployed and refueled by ISRU prior to the crew's arrival; then, the MALV the crew lands in can be refueled to serve as the ascent



vehicle for a subsequent crew mission.

As seen in Figure 4, in keeping with recent NASA Mars architectures, the mission concept considered in this initial assessment involves a short crew surface stay. [6] The roundtrip crew mission departing in 2039 follows an opposition class profile, sacrificing minimum energy transits for reduced total roundtrip time. In-space habitation for the crew is assumed to be provided by a dedicated Transit Habitat (TH), which is initially deployed and outfitted in a Lunar Near Rectilinear Halo Orbit (NRHO). A MIST vehicle is used to transport the TH through its full roundtrip Mars mission profile. The MALV in which the crew will land is assumed to deploy in the same year, using a non-minimum energy trajectory to arrive in Mars orbit just days before the crew.

Cargo MALVs are able to take nearly minimum energy trajectories in the 2037 Earth-Mars opportunity; however, in reality, cargo mission Earth departures will likely be staggered somewhat for operational/logistical reasons. Three landers are delivered in the 2037 opportunity; two cargo MALV vehicles outfitted with mobility, power, and ISRU equipment, and a third crew MALV to be refueled for crew ascent. Table 1 and Figure 5 lists the various payload pallets required to support one possible implementation of Mars surface ISRU operations, though other ISRU feedstock schemes and operations remain in the trade space [19], [20]. A stretched version of the MALV configuration may reduce the number of landers in the first opportunity by increasing payload volume and mass capability such that more payload pallets could be manifested on a single lander, but assessment of this option is not yet complete. In either case, an additional MALV is still required to deliver crew to the surface in the subsequent opportunity after the first MALV is fully replenished with propellants.

**Table 1 Borehole-Based kiloton Class Mars ISRU Manifest.**

300 mt Output Propellant Production Plant	QTY	Allowable Mass (kg)	Total Mass (kg)	Length (m)	Width (m)	Height (m)
<b>ISRU System</b>			<b>27,085</b>			
ISRU Plant Pallet	3	5,417	16,251	4.69	1.60	3.04
Liquifaction Pallet	2	3,500	7,000	4.69	1.60	2.94
Borehole Mining Pallet	2	1,917	3,834	4.69	1.60	2.42
<b>Power System</b>			<b>72,254</b>			
FSP Pallet	7	7,334	51,338	4.60	1.60	1.60
Controller Pallet	7	2,124	14,868	2.78	1.60	1.23
Cable/Converter Pallet	7	864	6,048	2.24	1.60 <td 0.85	
<b>Mobility System</b>			<b>12,707</b>			
Autonomous Chassis	3	3,467	10,401	5.01	3.39	1.12
Water Tanker	2	1,153	2,306	4.60	1.60	1.60
<b>Total Allowable Manifested Mass</b>			<b>112,046</b>			

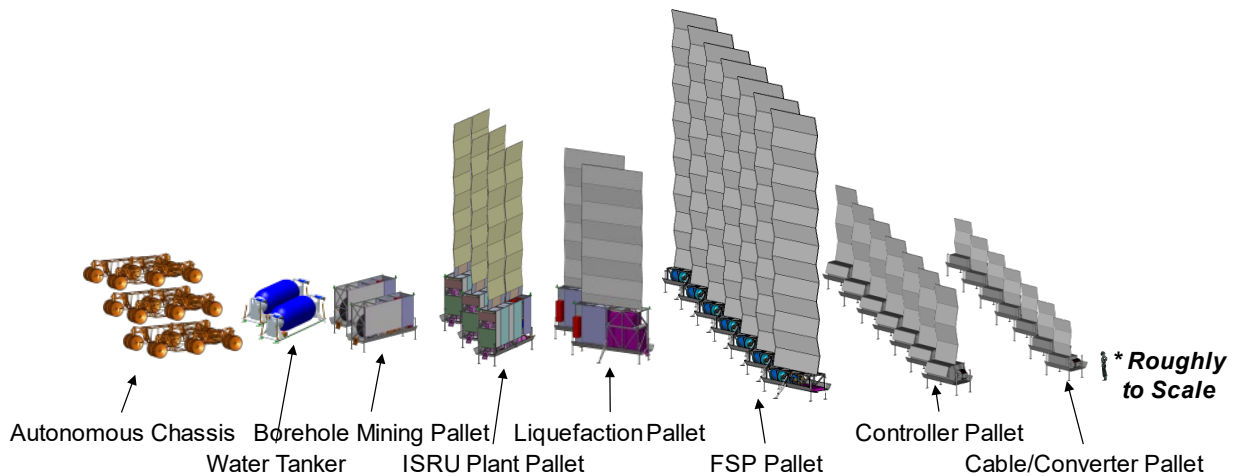


**Figure 5 Borehole-Based kiloton Class Mars ISRU Pallets, Radiators Deployed.**



The MALV and MIST vehicles rely on refueling in Earth orbit to execute their mission profiles. These orbital refueling services are assumed to be commercially provided, and their conops and logistics are not studied in detail here. After launch, the MIST and all four MALV vehicles are refueled in Low Earth Orbit (LEO). Depending on their mission profile, an additional refueling orbit may also be performed prior to Earth departure; this option is depicted in Figure 4 as the “Final Tanking Orbit.”

Sizing and synthesis results for the MACHETE concept are reported in the following sections. Section IV overviews the subsystem design considerations, and Section V provides a high-level summary of mission performance for the campaign described in this section.

## IV. Vehicle Systems

The following section describes in general the major subsystems of the transportation system. Not all configurations have all subsystems described below. The subsections that follow may also describe differences in the subsystems that exist for each of the vehicle configurations. As noted previously, assessment of a stretched version of the MALV is currently underway. Some characteristics of this additional MACHETE family member are called out in the discussion, but full integrated analysis of an architecture employing this variant will wait for a later publication.

### A. Configuration & Aerodynamics

The MALV has a spherically blunted tangent ogive nose cone and a cylindrical body, with the only major protuberances being the four landing leg fairings. This choice was made to maintain an outer mold line similar to many launch vehicle fairings, and represents a qualitative design compromise between EDL performance, Earth ascent performance, and launch vehicle integration. All vehicle configurations have an 8.4-meter outer diameter. Primary structures are maintained at 8.0 meters in diameter, allowing for 200 millimeters of additional thickness for thermal protection systems to be applied to the structure while still maintaining the 8.4-meter outer diameter. The MALV and MIST are 25.6 meters long from nose to engine exit plane. The MALV stretch configuration has a maximum length of 43.5 meters. The stretched configuration enables increased cargo bay volume, cargo capacity, and propellant capacity, but final sizing and performance analysis is not yet complete. A summary of key configuration parameters for all three variants can be found in Table 2.




To aid in providing aerodynamic stability and control authority during atmospheric entry, the MALV is designed with five body flaps positioned at the aft of the vehicle on the windward side. The flaps are stowed against the body of the vehicle, deployed for EDL as depicted in Figure 6, and stowed again during terminal landing. Flap sizing is currently notional, to be refined in future design iterations. Preliminary aerodynamic data was generated using CBAero for a range of dynamic pressure, Mach number, angle of attack, and flap deflection angle. This information was then used to perform preliminary EDL trajectory modeling to inform preliminary propellant mass estimates and provide a good initial dataset to support more detailed analysis of stability and control during EDL of such a vehicle geometry. This initial modeling was for an untrimmed trajectory, as it was performed before mass properties were available. With the completion of this initial design of the MALV, a more detailed EDL modeling effort was started, the results of which will be presented in a later publication.



**Figure 6 MALV Body Flap Deployment.**

The absence of the landing function from the MIST results in key configuration changes, such as no internal cargo bay or lift system, no landing systems, and no thermal protection system for aerodynamic entry. Additionally, the MIST has two large jettisonable panels: the aft engine section closeout ring, also used for launch vehicle integration, and the forward nose closeout. With the omission of landing legs, the aft closeout ring no longer is needed for landing system support and can be jettisoned to improve mission performance both from a mass and thermal perspective. The nose section is jettisoned to expose the forward docking mechanism as well as large solar arrays unique to the in-space stage configuration.

**Table 2 MACHETE Geometry and Capacity Summary.**

			
Configuration	MALV	MIST	MALV Stretch
Aerodynamic Shape	Spherically Blunted Tangent Ogive		
Outer Diameter (m)	8.4 meters		
Length (m)	25.6	25.6	43.5
Cargo Bay Volume (m <sup>3</sup> )	310	N/A	730
Cargo Bay Door Height (m)	4.7	N/A	4.7
Cargo Bay Door Width (m)	3.7	N/A	3.7
Cargo Lift Capacity (kg)	15,000	N/A	15,000
Main Fuel Tank Volume (m <sup>3</sup> )	175	350	270
Main Oxidizer Tank Volume (m <sup>3</sup> )	213	430	330
Header Fuel Tank Volume (m <sup>3</sup> )	18	N/A	55
Header Oxidizer Tank Volume (m <sup>3</sup> )	23	N/A	67
Cargo Capacity (kg)	75,000	50,000	150,000
Leg Deployed Diameter (m)	16.0	N/A	16.0

## B. Structures & Mechanisms

A full structural evaluation of each of the MACHETE configurations was performed using a series of finite element analysis tools including NX Patran, NX Nastran, and HyperSizer. An example mesh, including the cargo lift system, is shown in Figure 7. All primary structures assume metallic aluminum constructions, designed to NASA-STD-5001B with a yield strength factor of safety of 1.0 and an ultimate strength factor of safety of 1.4. [24] Aluminum was selected due to its low mass to strength ratio and overall, which have made it vital to many space systems in the past. However, because of the pre-phase A nature of the design, other factors that could drive alternative decisions on material selection were not performed, primarily, manufacturability and cost.



**Table 3 Load Case Summary.**

Config.	Load Case	Description	Loading			
			Propulsion	Main Tanks	Header Tanks	Payload [mt]
MALV [1,2,3,4]	1	Earth Ascent	MPS	Empty	Empty	75
	2	Earth-Mars Transit	MPS	Full	Full	75
	3	Mars EDL Initial	MPS	Empty	Full	75
	4	Mars EDL Final	LPS	Empty	Empty	75
	5	Mars Ascent Initial	MPS	Full	Empty	0
	6	Mars Ascent Final	MPS	Empty	Empty	0
MIST [5,6]	7	Earth Ascent	MPS	Empty	N/A	0
	8	Earth-Mars Transit Initial	MPS	Full	N/A	50
	9	Earth-Mars Transit Final	MPS	Empty	N/A	25
MALV Stretch [7,8,9,10]	10	Earth Ascent	MPS	Partial [11]	Empty	75
	11	Earth Ascent	MPS	Partial [11]	Empty	150
	12	Earth-Mars Transit	MPS	Full	Full	75
	13	Earth-Mars Transit	MPS	Full	Full	150
	14	Mars EDL Initial	MPS	Empty	Full	75
	15	Mars EDL Initial	MPS	Empty	Full	150
	16	Mars EDL Final	LPS	Empty	Empty	75
	17	Mars EDL Final	LPS	Empty	Empty	150
	18	Mars Ascent Initial	MPS	Full	Empty	0
	19	Mars Ascent Final	MPS	Empty	Empty	0

[1] MPS Thrust: 5 x 731 kN

[2] LPS Thrust: 4 x 211 kN

[3] Main Tanks Capacity: 290,000 kg (LCH4: 64,000 kg, LO2: 226,000 kg)

[4] Header Tanks Capacity: 35,000 kg (LCH4: 8,000 kg, LO2: 27,000 kg)

[5] MPS Thrust: 5 x 731 kN

[6] Main Tanks Capacity: 640,000 kg (LCH4: 149,000 kg, LO2: 429,000 kg)

[7] MPS Thrust: 5 x 1,256 kN

[8] LPS Thrust: 4 x 346 kN

[9] Main Tanks Capacity: 490,000 kg (LCH4: 114,000 kg, LO2: 376,000 kg)

[10] Header Tanks Capacity: 100,000 kg (LCH4: 23,300 kg, LO2: 76,700 kg)

[11] Exact propellant loading to be determined by Earth ascent performance analysis

A total of 19 load cases were evaluated across the three configurations. Table 3 lists the cases by configuration as well as relevant thrust, propellant, and payload information. The Payload masses listed in the table are not what the lift system is sized to, but rather the entire primary structure. Note the high number of load cases for the MALV stretch is due to the goal of developing parametric models of the concept. Having a set of data that independently varies the geometry and the payload mass impacts will support a more refined parametric model of the concept in both design dimensions.

The payload deployment mechanism was designed to 15,000 kg maximum static load for all configurations. The maximum mass of any single payload pallet plus a mobility system in the notional payload manifest in Table 1 fell under this load. Additionally, this mass resulted in static stability of both the MALV and MALV stretch configurations while offloading payload with up to a 10-degree tilt angle, when combined with the four leg 16-meter landing leg deployment diameter. This ensures that the vehicle will remain statically stable during payload offloading despite potentially uneven terrain. No analysis of dynamic landing stability has been performed; however, four legs is assumed to be a good balance between landing leg system mass and dynamic stability during touchdown.

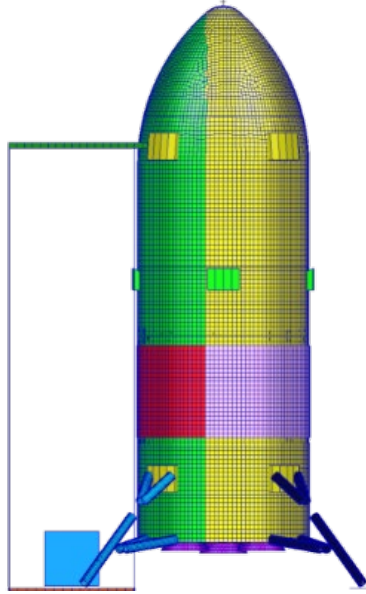


**Figure 7 MALV Structures FEM with Payload Deployment Mechanism.**

### **C. Propulsion**

The MALV propulsion system is oxygen/methane-based and highly integrated with multiple propellant tanks and engine systems all interconnected. The schematic in Figure 8 is a top-level depiction of the propulsion system. The vehicle concept consists of three engine systems: a main propulsion system (MPS), a landing propulsion system (LPS), and an attitude control system (ACS). The MPS supports all phases of flight except final touchdown. The LPS provide thrust for the final seconds of EDL just prior to touch down, as well as active tip over prevention after touchdown. The ACS is a methane cold gas blowdown system used primarily for pitch-yaw-roll control during in-space operations. There are three sets of propellant tanks: two liquid and one gaseous. The main propellant tanks are the largest, storing a bulk of the liquid propellant for all phases of flight except EDL. The main propellant tanks feed propellants to only the MPS. For EDL, a separate set of smaller header tanks are provided. These header tanks feed both the MPS and LPS during EDL only. The main purpose for a separate set of tanks for the EDL phase is to supply the engine systems with propellant from a more controlled environment experienced during the highly dynamic EDL phase of flight. This helps to minimize concerns related to propellant slosh and liquid acquisition. Finally, a set of composite overwrap pressure vessels (COPVs) provide storage of high-pressure gaseous propellants to be utilized by the ACS and fuel cell power system.

The concept lacks a traditional pressurization system because it employs autogenous pressurization via tap off from the MPS and LPS. The tanks required to store such vast quantities of traditional pressurant for such large propellant volumes would be prohibitive. High pressure gaseous fuel and oxidizer are tapped off of the MPS and LPS to pressurize their respective propellant feed systems. Fuel and oxidizer gases are kept separate and fed to their respective fuel and oxidizer tanks to prevent possible combustible mixtures forming within a given volume. Once a burn is complete, the gas introduced into the tank to maintain feed pressures during a burn are subsequently vented to remove excess heat from the ullage to minimize propellant loss due to boil off. This gas could be recaptured and stored for later utilization, however the flow rates to extract and store such vast quantities of ullage would result in massive power requirements on a pumping system. However, the concept does employ an ullage recouperation system to captures propellant that would otherwise be lost as boil off during long, quiescent phases of flight and repurposes it for utilization by the ACS and power system. This recaptured propellant is stored in the high pressure COPVs.

Preliminary mass fraction-based estimates, combined with optimal Mars ascent thrust to weight, resulted in a total required thrust of 2,280 kN at 380 seconds specific impulse. As the MALV concept was refined, the total thrust increased to 2,925 kN due to increased mass. To meet the required total thrust, The MPS consists of five gimbaled 731 kN engines, with a maximum exit diameter of 2.25 meters, laid out in a cross pattern similar to the Saturn V. Gimbaling of the main engines provide the necessary pitch and yaw control during supersonic retro propulsion. The number of engines was selected based on several design criteria and constraints. Five engines provide good engine out capability, as sets of engines can be deactivated to maintain stability in the event of a failure. There are only

vacuum optimized engines, as the vehicle does not operate under any significant ambient pressure that would benefit from optimizing to such exit conditions. Five engines also result in thrust per engine levels that are well within the bounds of historical engines designs such that existing engine turbomachinery designs, may be utilized.

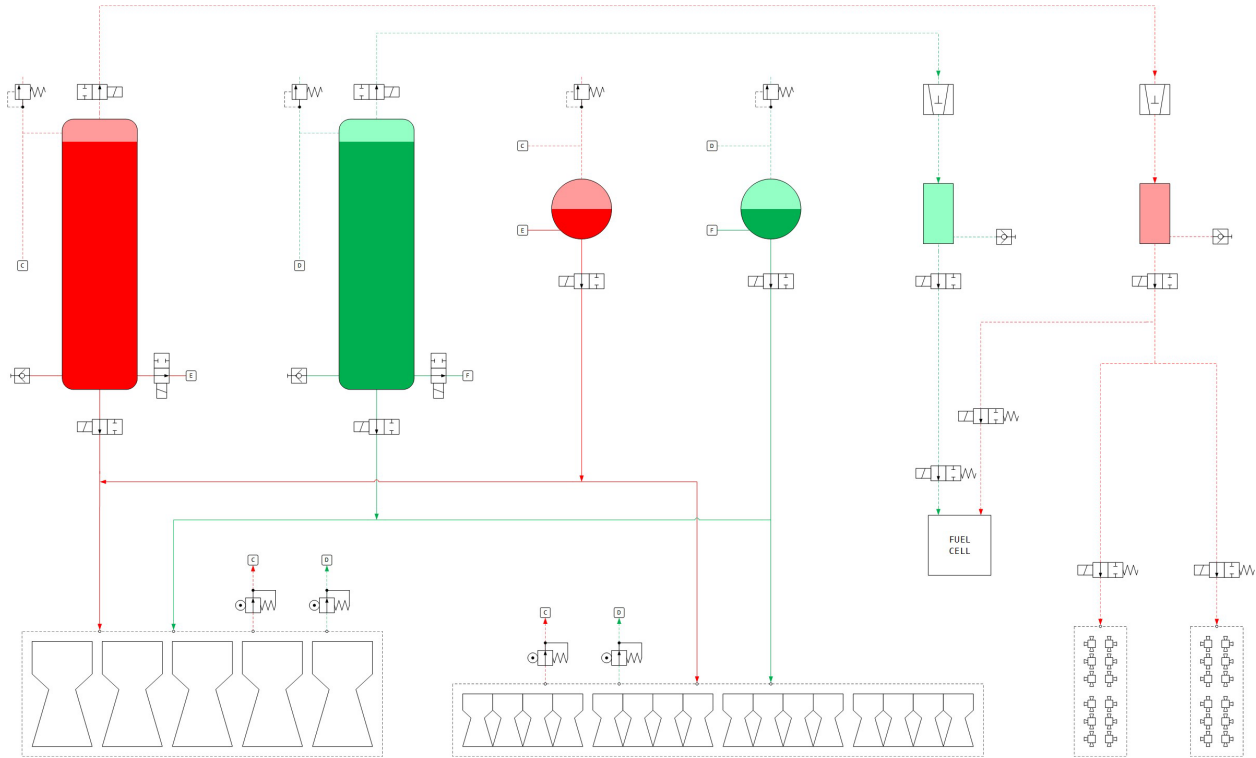


**Figure 8 Propulsion System Schematic.**

The MPS leverages highly advanced rotating detonation rocket engines (RDRE). These engines were selected for two primary reasons: extremely high performance in terms of specific impulse, and very short engines for the thrust level and performance. RDRE operate based on a pressure gain combustion process through the implementation of a rotating detonation wave, compared to a constant pressure deflagration combustion process implemented by all rocket engines flown to date. This allows RDRE to achieve significant performance increases while simultaneously reducing overall combustor and nozzle length. RDRE has the potential to improve engine specific impulse by as much as 10%-15%, reduce engine length by as much as 40%, and subsequently engine mass by as much as 30% over traditional constant pressure deflagration-based rocket engines. [25], [26] Without RDRE, the vehicle concept is not feasible. Both the reduction in engine length, combined with the improved specific impulse allow a vehicle geometry that fits within the constrained outer mold line desired, while allowing and ample cargo bay volume to house the payloads to support the initial human Mars mission concept assumed.

Preliminary analysis using ROCETS was performed on several different engine cycle designs for the MPS RDRE engines. Staged combustion was the initial choice for maximum performance. However, the higher injection temperatures resulting from the cycle were initially found to be outside the feasible ranges that a pressure gain detonation process could be sustained. The dual expander cycle was considered to reduce this high injection temperature, however, achieving a closed power balance was a challenge due to the required heat loads to power turbomachinery, specifically on the oxidizer side. The gas-generator cycle was ultimately selected as it did not exhibit the cycle power balance challenges observed in the other, higher performing engine cycles. However, achieving the required engine performance of 731 kN, 380 seconds specific impulse, and 2.25-meter exit diameter proved to be challenging for the lower performing gas-generator cycle. The schematic in Figure 9 is for the resulting MPS gas-generator RDRE engine concept. The schematic highlights specific valves used to control the engine's operation, as well as the nodes where gases are extracted from the engine to autogenously pressurize the feed systems during engine operation.



required was initially estimated to be 495 kN at 320 seconds specific impulse. However, as the MALV was refined and mass increased, the total LPS thrust required increased to 547 kN. Based on the engine schematic and layout discussed above, this resulted in four 211 kN engines, each with four 52.6 kN RDRE combustors. Similar to the MPS, this engine configuration supports engine out capability.

The discussion regarding propulsion up to this point has primarily focused on the MALV configuration. The primary difference with the MALV stretch is the increased mass resulting from the additional length. This results in higher required total MPS thrust, 5,023 kN, resulting in an engine thrust level of 1,256 kN. The increased mass also impacts the total LPS thrust to 900 kN, resulting in an engine thrust level of 346 kN. The primary challenge with the engine design compared to the lower thrust concept for the MALV is maintaining engine specific impulse under the same fixed 2.25-meter exit diameter. The increased flow rates to achieve the increased thrust are not as optimally expanded under the constrained exit diameter, resulting in slightly reduced engine specific impulse. For the MIST configuration, the thrust level required is significantly less than configurations that must ascend from the surface fully fueled. However, for commonality, the in-space configuration maintains the same five 731 kN MPS engine configuration as the MALV. The LPS and header tanks are removed from the MIST to maximize the main tank propellant capacity required to perform the round-trip mission to and from Mars.

#### D. Power

The MALV concept considered a variety of alternative power system architectures. A system based entirely on oxygen-methane fuel cells to produce the required power for the entire mission duration was first studied. Oxygen-methane fuel cells were selected for the obvious commonality of the reactants with the propulsion system. The reactants for the fuel cells would be scavenged from propellant ullage over the course of the mission, stored and supplied by the COPVs as discussed under the propulsion subsystem section. The fuel cell power architecture consists of five parallel fuel cells connected to two parallel power distribution units, each providing a 120 volt and 28 volt output, shown in Figure 11(a). A summary of the power budget for primary outbound mission phases can be found in Table 4, while Mars ascent power budget is found in Table 5. All units are in Watts unless otherwise noted. The peak power experience during Mars descent and ascent are the sizing mission phases at 12,644 peak Watts required by the fuel cell power plants. The out bound power budget results in roughly 22,000 kg of reactants to supply power for that leg of the mission. Mars ascent, because of its much shorter overall duration, only requires about 700 kg of reactants.

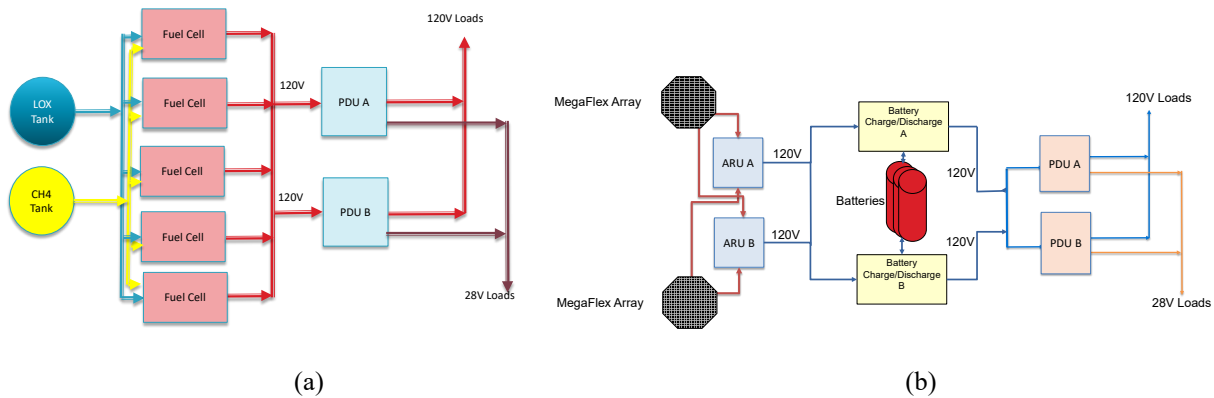


**Figure 11 Power System Architectures. (a) Fuel Cells. (b) Solar Arrays with Batteries.**

The vast quantity of reactants required to supply power for the longer coast phases of the mission led to alternative power systems being considered, particularly to support the MIST configuration. A purely Solar array-based power systems is shown in Figure 11(b). This system helped two-fold with performance, as it slightly increased the usable propellant while simultaneously significantly reducing the inert fluid mass that is bookkept, at the cost of a minimal dry mass impact for solar panels and batteries.

There are slight differences in the power system depending on the configuration. The MALV has only a fuel cell power system, shown in Figure 11(a). A combined fuel-cell and solar array power system architecture was studied for the MALV. However, though it did reduce the total propellants of the outbound flight, the increased dry mass associated with the solar arrays and batteries drove an increase in ascent propellant demand. Because ascent propellant demand is also the main design parameter affect ISRU system design, minimizing this propellant load took precedent,

leading to an all-fuel cell-based power system architecture for the MALV. The MIST power system architecture, shown in Figure 11(b), does not contain a fuel cell power system component, because it does not operate in environments where solar array cannot be deployed. The MIST also must provide additional power to support the Mars Transit Hab. This results in roughly a 12,000-Watt additional load that must be supported while in Mars orbit. Because of  $R^2$  losses at Mars distance, the net impact to solar array area is significant, resulting in two 11-meter diameter MegaFlex arrays stowed in the forward nose section of the vehicle, providing a total 180 square meters of solar arrays when deployed.

**Table 4 Power Profile During Earth-Mars Transit and EDL.**

Source	Launch	Propulsion	Coast	AR&D	Descent	Surface
Duration(hrs)	1	2	6224	4	1	24
ACS	78.5	78.5	70.5	720.5	559.5	0.0
C&DH	674.4	893.0	734.6	923.0	893.0	734.6
Comm	145.4	451.8	676.8	534.0	559.4	658.1
Sys Ctl	882.1	1072.6	778.2	800.6	1290.6	748.2
MPS	0.0	5280.0	0.0	0.0	5280.0	0.0
RCS	0.0	915.0	345.0	345.0	915.0	0.0
Thermal	0.0	1758.0	1758.0	1758.0	1758.0	1758.0
ECLSS	0.0	0.0	0.0	0.0	889.4	889.4
Crew Systems	0.0	0.0	0.0	0.0	500.0	500.0
<b>Total</b>	<b>1780.4</b>	<b>10448.9</b>	<b>4363.1</b>	<b>5081.1</b>	<b>12644.9</b>	<b>5288.3</b>
Growth (30%)	534.1	3134.7	1308.9	1524.3	3793.5	1586.5
<b>Predicted Power</b>	<b>2314.5</b>	<b>13583.6</b>	<b>5672.0</b>	<b>6605.4</b>	<b>16438.4</b>	<b>6874.8</b>

**Table 5 Power Profile During Mars Ascent to 5-sol.**

Source	Surface	Ascent Propulsion	Ascent Coast
Duration(hrs)	24	1	119
ACS	0.0	559.5	70.5
C&DH	734.6	893.0	734.6
Comm	658.1	559.4	676.8
Sys Ctl	748.2	1290.6	778.2
MPS	0.0	5280.0	0.0
RCS	0.0	915.0	345.0
Thermal	1758.0	1758.0	1758.0
ECLSS	889.4	889.4	889.4
Crew Systems	500.0	500.0	500.0
<b>Total</b>	<b>5288.3</b>	<b>12644.9</b>	<b>5752.5</b>
Growth (30%)	1586.5	3793.5	1725.8
<b>Predicted Power</b>	<b>6874.8</b>	<b>16438.4</b>	<b>7478.3</b>

## E. Avionics

Avionics include command and data handling, communication, and tracking, as well as guidance, navigation, and control for all phases of flight. All critical avionics systems are assumed to be two fault tolerant. It should be noted that the design of the MALV avionics does not support direct to Earth communication during EDLA. It is dependent on other orbital assets, such as the Mars Transit Habitat, in-space transportation vehicle, or communications relays, to communicate back to Earth during these phases of flight. The general communications approach is shown graphically in Figure 12.

The avionics subsystem concept utilizes mostly heritage hardware, such as Orion-derived flight controls for crew interface, as well as a Moog/Broad Reach suite as the baseline. EDL utilizes a terrain relative navigation system, similar to that found on the Mars 2020 lander, consisting of lidar altimeters, a lander vision system, and hazard avoidance sensors. The MALV is assumed to be the active vehicle during autonomous rendezvous and docking with other architecture elements. However, the MIST will act as the passive vehicle when docking with the Mars Transit Habitat. The concept contains X, S, and C-band communications equipment to support various vehicle functions. X-band is primarily utilized for high data rate telemetry and video to the near-Earth network, deep space network, and communication satellites. It has a maximum data rate of 400 Mbps. S-band communications are used for near-space network telemetry and tracking, communication during EDLA and surface to orbit operations around Mars, communication with other architectural elements, and during autonomous rendezvous and docking operations. The S-band is capable of up to 50 Mbps for telemetry with the near-space network, 50 kbps with other architectural elements,



8 Mbps for inter-surface telemetry and video, and 100 kbps during docking operations. The C-band is primarily used for range safety and docking operations. The vehicle does not contain Ka-band communications because of challenges associated with dish pointing during EDLA.

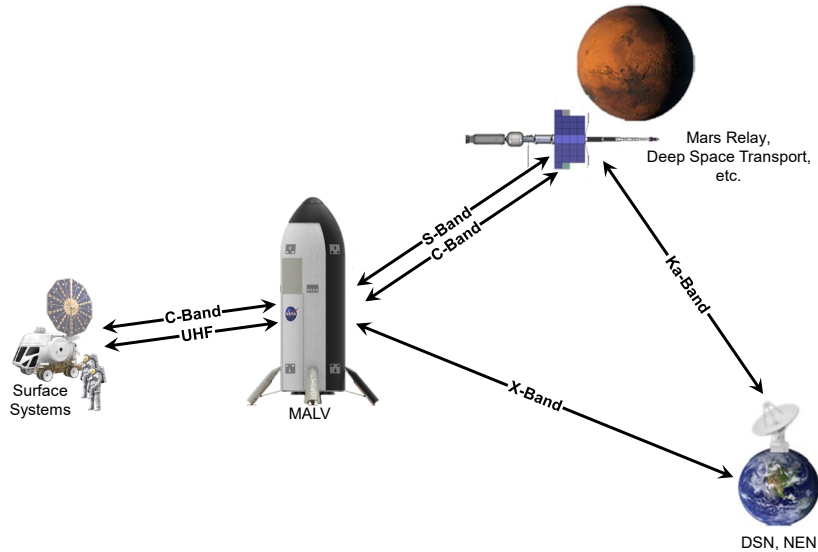


**Figure 12 MALV Communication Architecture.**

#### **F. Thermal Protection & Management**

The MALV thermal subsystem is a highly complex, integrated concept with several constraints including: 1) minimize boiloff from the methane and liquid oxygen tanks during transit, 2) maintain components above their survival temperature limits during quiescent phases, 3) provide a heat sink to prevent the other subsystems from overheating, 4) insulate from aerothermal heating during Mars EDL and 5) insulate the tanks during liquefaction on Mars. The constraints on the MIST are the same except without constraints 4 and 5, and with the additional constraint that the MIST vehicle's engines are pointed to the sun to accommodate the needs of the Mars Transit Habitat.

Liquid oxygen can be stored at up to 100 K (37 psia ullage pressure) and liquid methane can be stored up to 124 K at the same pressure. The two tanks share a nested bulkhead (parallel and offset bulkheads with MLI between) to make it possible to store or liquify the propellants at different temperatures. The MALV configuration can passively store the cryogenic propellants during transit simply by pointing the vehicle's nose towards the sun to minimize the projected area of the vehicle with respect to the sun and thereby minimize solar heating. This is true for the MALV's aspect ratio, but could become untrue if the MALV becomes shorter, because a shorter MALV will have less surface area to radiate heat while having the same projected area (unless the diameter also goes down). The MIST configuration is more challenging because the vehicle must point engine to sun. This orientation puts solar heating on the liquid oxygen side of the vehicle and puts the engine nozzles (which will not have optimal optical properties) directly in sunlight. Thermal Desktop modelling indicates the MIST configuration will require 2 cryocoolers (plus a spare) to maintain the liquid oxygen below 100 K. This compares favorably to the MIST configuration containing the aft skirt which required 7 cryocoolers (plus a spare). As seen in Figure 13 and Figure 14, the aft skirt is relatively hot and causes the engines to be hotter as well, because the aft skirt is acting like a light trap that blocks sunlight reflected off the LOX tank and gives the sunlight multiple passes at absorption. Additionally, the aft skirt blocks the engine's thermal radiation to deep space.

The vehicles include temperature sensitive hardware such as electronics, cryocoolers, and valves that must be maintained within their required temperature limits. This is accomplished with structural radiators, heaters, wiring, and thermostats. The power used to maintain temperatures is documented in the power section, and the masses are included in the mass summary.

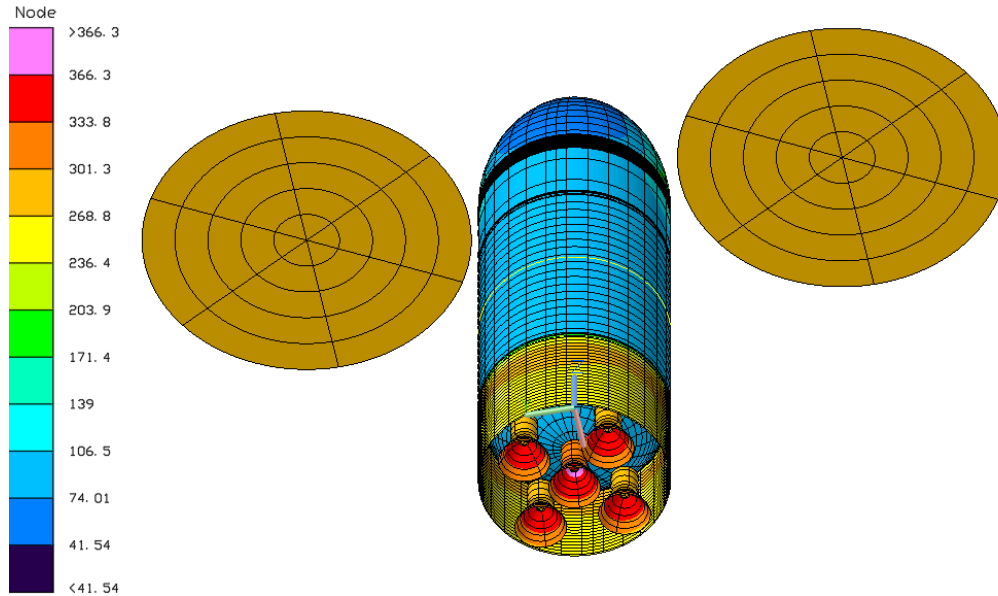


**Figure 13 MIST Thermal Desktop Model, Tail to Sun during transit with Aft Skirt Attached.**

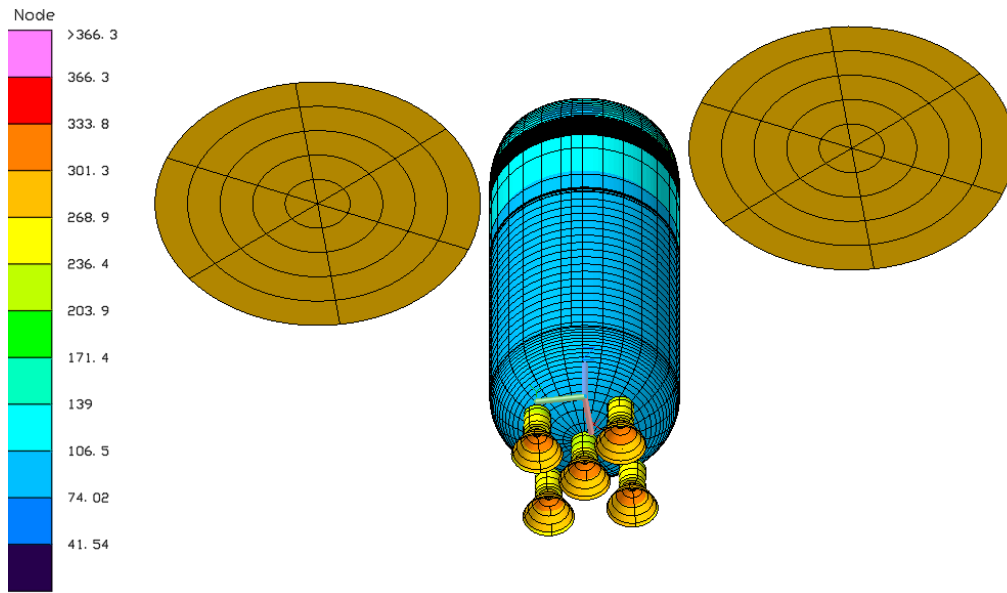


**Figure 14 MIST Thermal Desktop Model, Tail to Sun during transit without Aft Skirt.**

The tanks' Thermal Protection System concept is designed to survive the harsh environment experienced during Mars atmosphere entry and flight, while also being able to store vast amounts of cryogenic fluids during deep space flight and refueling on the Martian surface. To achieve this, the thermal protection system (TPS) of the MALV concept utilizes two layers of thermal protection: an outermost reusable component mounted to a stiffened Multi-Environmental Multi-Layer Insulation (MEMLI). [27], [28] The windward side of the vehicle uses a tile-based Toughened Uni-piece Fibrous Reinforced Oxidation Resistant Composite (TUFROC), resulting in the distinctive black belly. [29] The leeward side utilizes an Advanced Flexible Reusable Surface Insulation (AFRSI) like those used on the Space Shuttle Orbiter. Figure 15 depicts the notional layered TPS concept. The exact thicknesses of TUFROC and AFRSI components are yet to be determined precisely, as this depends on more detailed EDL flight mechanics modeling that has yet to be completed. Initial estimates for thicknesses were based on Space Shuttle reentry heating loads. Note, the MIST configuration does not require the outmost TPS layer, since it does not perform Mars EDLA.

For sections of the vehicle covering the main propellant tanks, the MEMLI consist of a broad area cooling network with a multi-layer insulation (MLI) with rigid spacers for optimized thermal performance. The composite sandwich shell consists of IM7 face sheets with aluminum honeycomb core. This composite acts as both a vacuum jacket over the broad area cooling network and MLI, as well as the main support structure for the outermost reusable TPS components. This composite structure is highly rigid to support the TUFROC material, which must maintain a maximum radius of curvature of 0.0025 inches to prevent cracking and separation of the tile-based protection system. For sections of the vehicle other than the main propellant tanks, where there is no need for the broad area cooling and MLI, the outer reusable TPS layer is supported by just the honeycomb composite shell to maintain a smooth outer mold line over the entire vehicle.

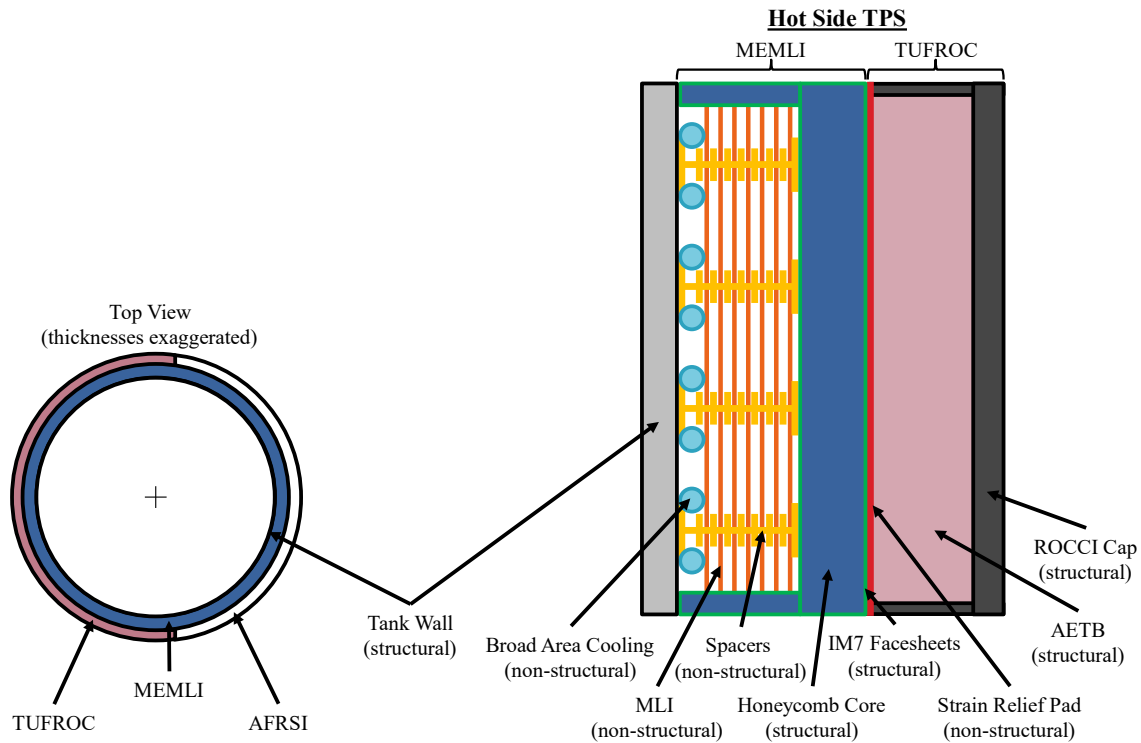


**Figure 15 Thermal Protection System Concept (Thicknesses Not to Scale).**

### G. Crew Support

Unique to the MALV configuration is an integrated crew cabin in the nose of the vehicle. The cabin is designed to support crew for 84 hours nominally with capability for 5-days contingency. The cabin has ample room for two crew with sleeping quarters, a gally, and latrine, as well as workspaces and storage for sample freezers and logistics containers. A subfloor provides storage for crew support related subsystems such as environmental control and life support systems and crew flight control avionics.

The crew cabin provides crew ingress and egress to other docked elements through a forward docking port, while also providing an access hatch in the floor for crew access to the payload bay. The forward docking port conforms to the NASA Docking System Block 2 interface definition, which is a draft update to the interface definitions of the Block 1 standard [23]. The cargo bay access hatch is similar to the 50 x 50 inch Common Birthing Mechanism hatches on the International Space Station. A pressurized tunnel can be outfitted to allow for shirt-sleeve transfer of crew to and from integrated payloads, such as a pressurized rover shown in Figure 16(a), while helping prevent uncontained Martian material from entering the crew cabin, and ultimately back contamination of Earth. Figure 16(b) highlights a notional 2-crew cabin layout. Other Mars ascent vehicle configurations studied are specially designed for a given number of crew. [13] Any changes to that number of crew can have drastic impacts on the overall design and mass of the vehicle concept. However, due to the relatively large dry mass of a vehicle of this scale, combined with the large volume present in the nose structure, increasing accommodations for up to six crew is feasible with minimal design change or impact to the MALV concept.

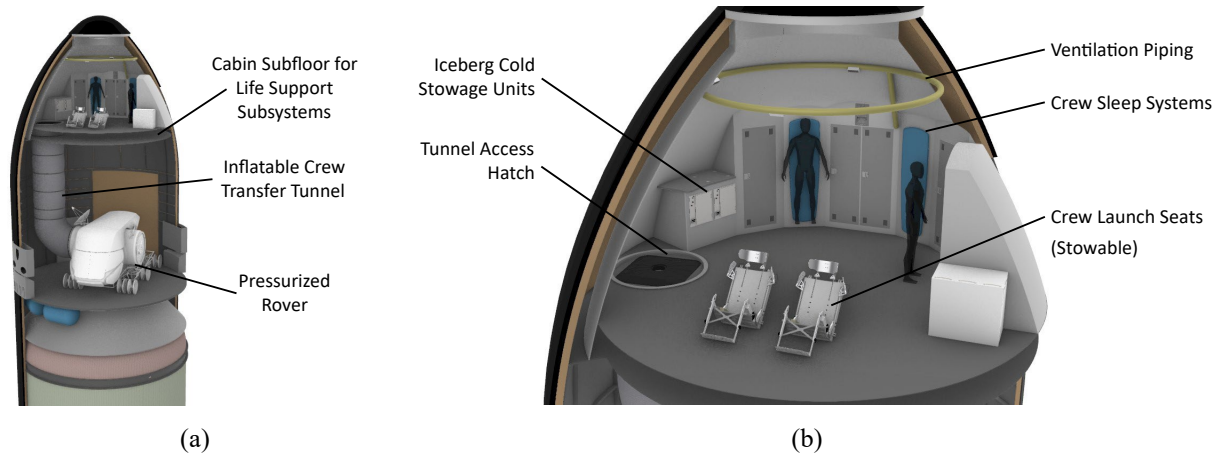


**Figure 16 Concept Images of MALV Crew Cabin and Payload Bay Access. (a) Shirt-sleeve Transfer Configuration for Crew Surface Access. (b) 2-Crew Capacity Cabin Configuration.**

The environmental control and life support system consist of several major components include the pressure control system (PCS), air revitalization system (ARS), particulate control, emergency management system (EMS), temperature and humidity control, and waste management system (WMS). Due to the limited crew duration, certain human factors items were omitted, such as exercise equipment and food warmers. Crew provisions include items such as food bars and drink bags, tool kits, towels and hygiene supplies, trash bags, fecal collection and cleaning supplies, and personal provisions. These items total to roughly 30 kg per crew member. Several of these items are expected to be transferred to the MALV after the crew arrives at Mars due to storage duration limitations of perishable items. Safety gear include items such as medical kits, personal radiation dosimeters, cabin illumination, and restraints. Each crew member is provided a sleeping system which includes a sleeping bag, cushion, pillow, and restraint. It is expected that sleeping will only be in a microgravity environment. A mass, power, and thermal allocation is also provided for utilization, to encompass scientific sample return and any stowage systems.

## V. Mission Performance

This section covers vehicle performance and includes discussions on in-space flight performance, Mars entry descent, landing, and ascent flight performance, preliminary campaign performance, and vehicle mass properties. These performance results ultimately drove initial estimates for a Mars surface ISRU system in the architecture concept. Several tools were utilized to perform the various analyses and data discussed in this section. The Program to Optimize Simulated Trajectories II (POST2) provides capabilities to target and optimize point mass trajectories for multiple powered or un-powered vehicles near and arbitrary rotating, oblate planet. This is ideal for modeling planetary entry, descent, landing, and ascent, including atmospheric flight. Dymos, a multi-disciplinary optimal control library, was utilized for preliminary EDL modeling [30]. Copernicus, a generalized spacecraft trajectory design and optimization system, is primarily used for exoatmospheric trajectory design and optimization. Dyreqt provides a general capability for synthesis of space systems and system-of-systems architectures in the pre-conceptual and conceptual phases of design. Rather than focusing on sizing, the primary aim of Dyreqt is enabling flexible synthesis of any arbitrary architectures that may be described within Dyreqt's ontology. In doing this, Dyreqt enables the rapid exploration and optimization of concepts subject to parametric constraints regardless of the high-/low-/mixed-/multi-fidelity nature of the disciplinary models used [31], [32]. Here, Dyreqt is utilized for the preliminary propellant mass estimation across the entire campaign.

## H. In-space Flight Performance

A Copernicus model was used to develop a set of reference trajectories shown in Table 6. The reference trajectories are ballistic with an inbound deep space maneuver. The trajectories target a total duration of 850 days from Earth departure to Earth arrival, though some opportunities result in slightly less time. A few assumptions are made for all trajectories to accommodate various mission operations. Roughly 10 days post-Mars arrival and pre-Mars departure allow for orbital operations before and after the surface mission. The surface mission is fixed at 30 days resulting in roughly 51 days total time in Mars orbit. On top of the 850 days, 10 additional days are maintained pre-Earth departure

and post-Earth arrival to account for various crew operations at either end of the mission. Finally, and additional 90 days before Earth departure are maintained to allow for crew to launch from Earth.

Minimum energy Earth-Mars departure opportunities are given between 2037 and 2052. The minimum  $\Delta V$  opportunity in this period occurs in the 2050 opportunity, while the maximum  $\Delta V$  opportunity occurs in the 2043 opportunity. The architecture concept presented requires Earth departures during two separate opportunities. The 2037 and 2039 opportunities were chosen for this analysis as they represent a compromise between the minimum and maximum  $\Delta V$  opportunities. Because the cargo mission must fly before the crew mission, the cargo sortie flies the 2037 opportunity, and the crew sortie flies the 2039 opportunity. The  $\Delta V$  associated with these opportunities are used to estimate propellant loads which influence vehicle sizing, ISRU demand, and ultimately, overall campaign performance.

**Table 6 Type A (Inbound Deep Space Maneuver) High Thrust Ballistic 850 Day Earth-Mars-Earth Reference Trajectories**

Reference Type A	High Thrust Ballistic 850d EME	High Thrust Ballistic 850d EME	High Thrust Ballistic 850d EME	High Thrust Ballistic 850d EME	High Thrust Ballistic 850d EME	High Thrust Ballistic 850d EME	High Thrust Ballistic 850d EME	High Thrust Ballistic 850d EME	
	2037	2039	2041	2043	2046	2048	2050	2052	
Earth Departure	09/01/2037	10/20/2039	11/19/2041	12/28/2043	02/09/2046	04/01/2048	05/29/2050	08/06/2052	
Deep Space Maneuver	11/20/2037	03/11/2040	06/03/2042	06/02/2044	06/09/2046	06/20/2048	11/11/2050	11/30/2052	
Mars Arrival	04/05/2038	07/06/2040	08/24/2042	08/25/2044	09/13/2046	10/19/2048	12/16/2050	02/24/2053	
Mars Departure	05/26/2038	08/27/2040	10/14/2042	10/15/2044	11/03/2046	12/25/2048	02/06/2051	04/17/2053	
Deep Space Maneuver	03/06/2039	05/22/2041	05/17/2043	05/30/2045	06/26/2047	09/13/2049	01/14/2052	02/18/2054	
Earth Arrival	11/23/2039	02/16/2042	03/18/2044	04/26/2046	06/08/2048	07/30/2050	09/24/2052	11/06/2054	
Outbound	216.0	260.5	278.5	240.3	215.4	200.9	201.2	202.2	
Stay	51.0	51.7	51.3	51.3	51.5	67.2	51.5	51.5	Days
Inbound	546.0	538.4	520.2	558.4	583.0	581.9	596.4	568.6	
Total	813.0	850.6	850.0	850.0	850.0	850.0	849.1	822.3	
Crew Launch Window	90	90	90	90	90	90	90	90	
Pre-Departure	10	10	10	10	10	10	10	10	Days
Post-Arrival	10	10	10	10	10	10	10	10	
Total Off Earth	923.0	960.6	960.0	960.0	960.0	960.0	959.1	932.3	
Trans-Mars Injection	928.20	1,230.45	910.49	1,020.99	972.88	658.73	453.85	768.84	
Deep Space Maneuver	0.00	0.00	0.23	0.64	0.00	0.00	0.83	0.32	
Mars Orbit Insertion	916.10	857.63	883.63	1,225.24	1,416.39	1,297.25	977.25	912.46	m/s
Trans-Earth Injection	733.30	844.18	1,226.57	1,006.63	855.68	836.34	500.26	504.57	
Deep Space Maneuver	2,309.30	2,841.20	2,544.97	2,326.16	1,946.00	1,551.37	1,844.12	2,215.28	
Earth Orbit Insertion	801.50	626.35	894.35	1,013.62	1,053.56	980.73	829.46	825.24	
Total DV	5.6884	6.3998	6.4602	6.5933	6.2445	5.3244	4.6058	5.2267	km/s

### I. Mars Entry, Descent, Landing, and Ascent Performance

A preliminary analysis of Mars entry, descent, and landing was performed by developing a simple two degrees of freedom model in the vertical and longitudinal coordinates. The main objective of the analysis was to obtain an initial estimate of EDL  $\Delta V$  to aid with preliminary mass estimation. A representation of the EDL concept of operations is given in Figure 17. The trajectory was broken into four phases of flight for the preliminary analysis: fixed angle of attack initial entry, active pitch control, reorientation, and powered descent. Reorientation was modeled as an instantaneous change in angle of attack, and the terminal descent phase assumed a constant velocity vertical descent. For an initial mass of 185,000 kg, and propulsion parameters as described in Section IV.C, powered descent was predicted to require 738 m/s. However, given the low fidelity of the model and the omission of modeling the reorientation maneuver, a factor of 1.2 was applied to this value for preliminary mass estimation. For a fixed velocity terminal descent, the total  $\Delta V$  can be estimated purely as a function of time. Assuming a 2 m/s vertical velocity and terminal phase initiation at 30 meters altitude requires 15 seconds to descend. Adding an additional 10 seconds of hover for hazard avoidance results in a total 25 second terminal phase, countering the local Mars surface gravitational acceleration of 3.72 m/s<sup>2</sup> over this duration results in a total 93 m/s velocity change for terminal descent. Higher fidelity models are actively being developed to better study the EDL flight mechanics of such a concept, particularly the reorientation phase and landing accuracy.

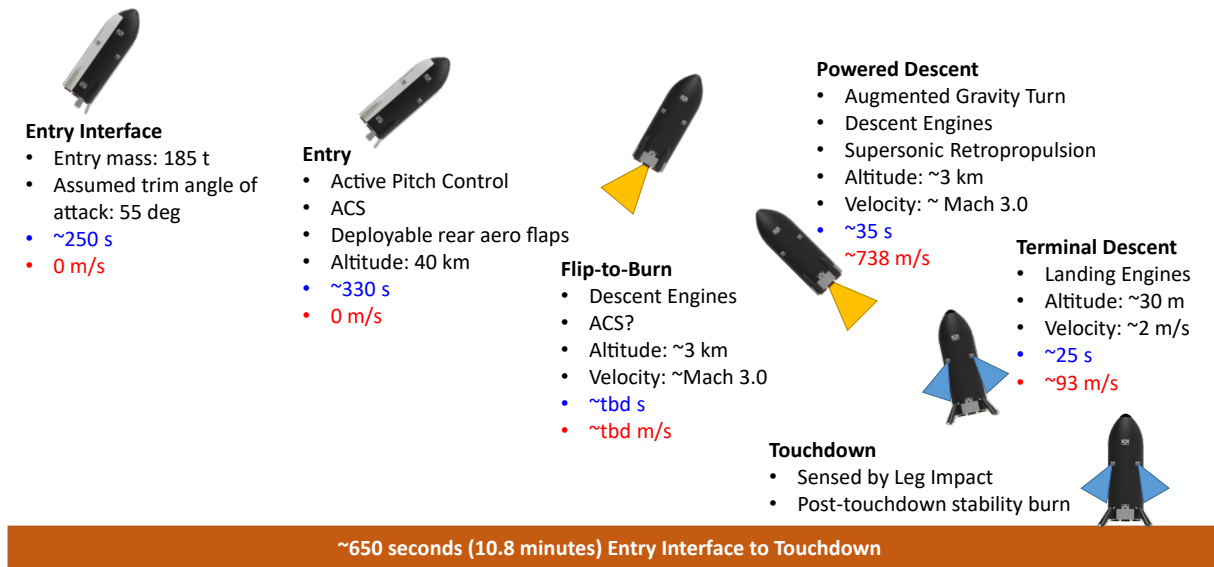


Figure 17 EDL Concept of Operations

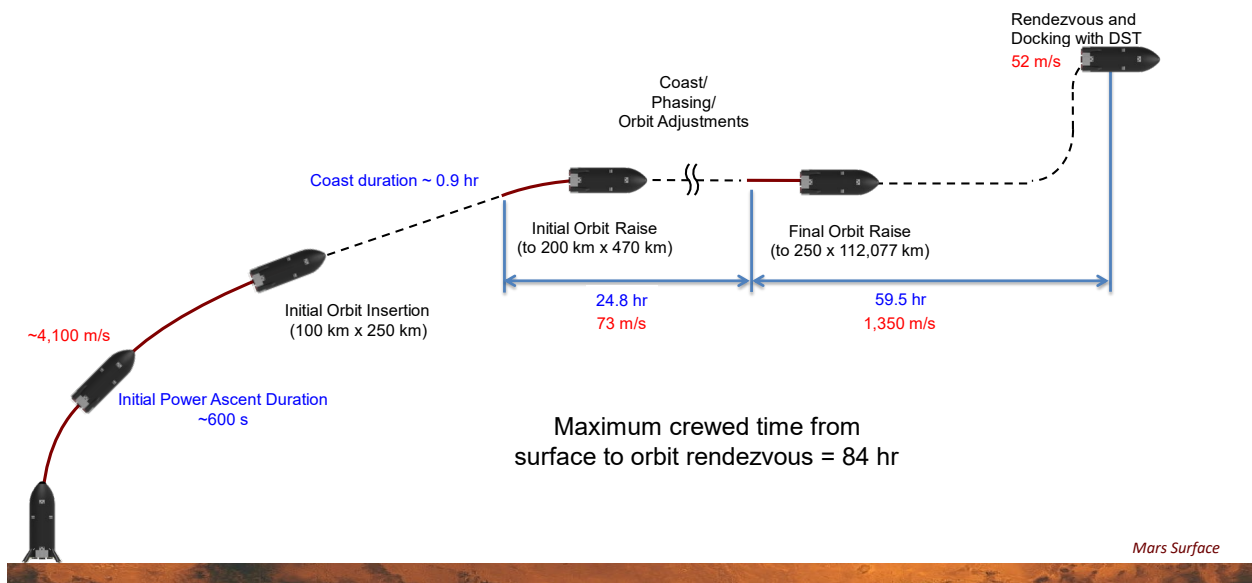


Figure 18 Mars Ascent Trajectory to 5-sol, Overview

Ascent from the surface of Mars is performed over a series of burn and coast maneuvers as depicted in Figure 18. An initial powered ascent phase of roughly 600 seconds propels the vehicle to an initial low Mars orbit of 100 km by 250 km. A short coast phase occurs before performing a series of orbit raise burns to an intermediate phasing orbit 200 km by 470 km. After a 25-hour phasing period, a final orbit raise maneuver is performed into a 250 km by 112,077 km coelliptic orbit with the target 5-sol orbit. A final coast phase of roughly 60 hours occurs before performing final termination phase burns, rendezvous, and docking. The series of in-space burns performed to rendezvous with the target 5-sol orbit are derived from historical Apollo, Shuttle, and Orion flight operations [33].

A POST2 model was developed to model the initial power ascent to 100 km by 250 km circular. An initial Earth thrust to weight versus total ascent  $\Delta V$  curve from a notional landing site of Deuteronilus Mensa (43.9 degrees North latitude, 22.6 degrees East longitude) to the initial park orbit of 100 km by 250 km altitude was generated with the model. The resulting data is shown in Figure 19. clearly has a minimum  $\Delta V$  solution at 0.75 initial stage Earth thrust to weight ratio of 4,143 m/s. A Copernicus model was used to predict the trajectory from initial orbit insertion to 5-



sol. The resulting transfer trajectory resulted in a  $\Delta V$  of 1,429 m/s beyond the initial powered ascent to 100 km by 250 km. The total ascent  $\Delta V$  from Mars surface to 5-sol is then 5,572 m/s. Mars Ascent results in the bounding propellant load demand for the concept. This ultimately drove engine thrust levels in an effort to minimize total ascent  $\Delta V$ . The resulting propellant load is also the primary driver for the Mars surface ISRU systems.

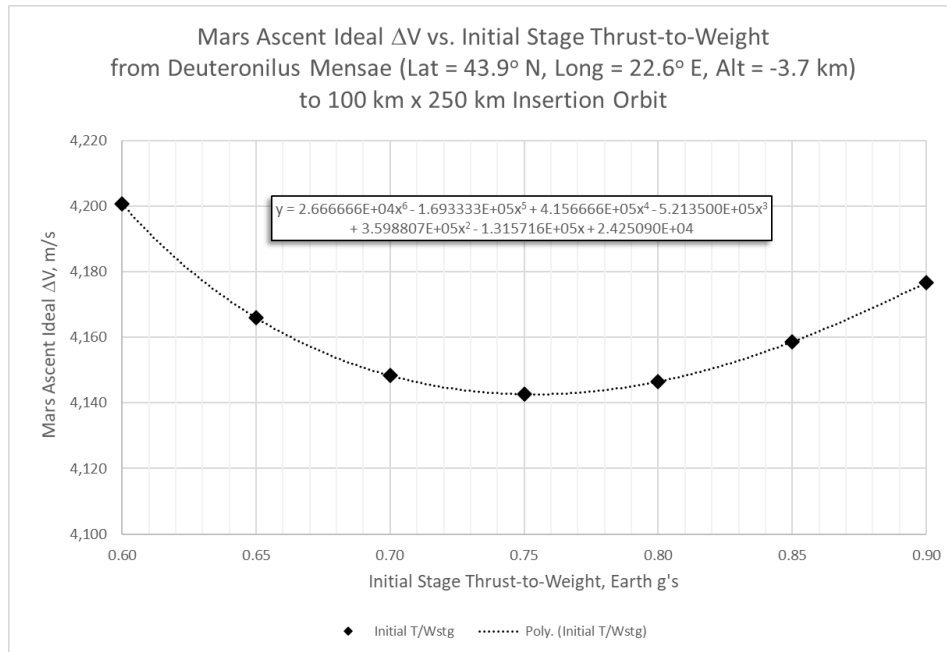


**Figure 19 Ascent  $\Delta V$  to Low Mars Orbit vs. Initial Thrust to Weight Ratio for a Single Stage Ascent Vehicle**

## J. Campaign Performance

Utilizing the  $\Delta V$  data discussed in the previous subsection, preliminary estimates of propellant and mass were obtained for the architecture concepts given in Figure 4. The manifest of payload to be delivered for the Mars surface ISRU system are given in Table 7. Note, the manifested payloads in this table result in significantly lower total payload mass than the assumed 75,000 kg payload capacity of the MALV concept. Although the MALV has a sizable cargo bay and landed mass capability, preliminary designs of the ISRU and power equipment resulted in the cargo bay being volume limited well before mass limits were met. The campaign analysis in this section assumed missions start and end in Earth orbit. Details regarding deliver to Earth orbit, propellant supply from Earth prior to trans-Mars injection, alternative aggregation orbits, or alternative concepts of operation are out of the scope of this paper. Rather, the primary objective was to detail the source for a propellant load estimate that ultimately bounds the ISRU production capacity to support the notional architecture.

The same analysis was performed for data generated in both the initial design analysis cycle (DAC1), as well as the subsequent design analysis cycle (DAC2). DAC1 was the initial concept design development of the MACHETE family of concept while DAC2 refined these concepts. Additionally, select subsystem architecture trades were evaluated based on observations from DAC1, including and alternative power system architecture, and increased thrust engine concepts to support increased masses as the concepts evolve. Analysis of the MALV concept from DAC1 provided the initial estimate of the quantity of propellant the ISRU system would have to generate to support the architecture concept. Table 8 lists the various propellant masses across major events. The most relevant propellant quantity in bounding the ISRU production demand is that associated with refueling the MALV for ascent from the surface of Mars. DAC1 data resulted in roughly 309,000 kg of propellant to perform Mars ascent. These results ultimately dictate the 300,000 kg production capacity for the Mars surface ISRU systems in the architecture concept.

**Table 7 Notional Campaign Lander Manifesting**

300 mt Output Propellant Production Plant	QTY	Allowable Mass (kg)	Lander Manifest		
			Lander 1	Lander 2	Lander 3
<b>ISRU System</b>					
ISRU Plant Pallet	3	5,417			3
Liquifaction Pallet	2	3,500			2
Borehole Mining Pallet	2	1,917		2	
<b>Power System</b>					
FSP Pallet	7	7,334	5	1	1
Controller Pallet	7	2,124	5	1	1
Cable/Converter Pallet	7	864	5	1	1
<b>Mobility System</b>					
Autonomous Chassis	3	3,467	1	1	1
Water Tanker	2	1,153		2	
<b>Total Allowable Manifested Mass</b>			<b>55,077</b>	<b>19,929</b>	<b>37,040</b>

A primary driver for DAC2 was to refine the MACHETE vehicle concept to show a feasible architecture. The MIST, utilizing only fuel cell power resulted in excessive propellant loads that were infeasible. To mitigate this, a solar-based power system was designed for MACHETE. Outfitting the MIST with solar power, drastically reduced the total propellant load, shown in Table 9, resulting in a feasible concept. The same solar array-based power system was also outfitted on the MALV to reduce the amount of propellant inventory used for power generation, to improve mission performance. This resulted in lower propellant loads required for the outbound flight. However, the added dry mass of the solar power system resulted in increased Mars ascent propellant requirements. This is because, the total ascent duration of 84 hours does not require significant amounts of fuel cell reactants, less overall mass than a solar power system incurs. This is just one example of nuanced design details that only show up when performing full campaign analysis. Numerous other emergent trends are likely to arise when expanding the campaign analysis to include additional phases of the mission going all the way back to Earth launch and alternative architecture concepts.

**Table 8 Notional Campaign Major Event Mass History by Element, DAC1**

Mission	Opportunity	Vehicle Configuration	Mass Category	Event Masses, [Mg]								
				Trans-Mars Injection	Mars Orbit Insertion	Mars EDL	Mars Apotwist	Mars Ascent	Trans-Earth Injection	Deep Space Manuever	Earth Orbit Insertion	
Cargo Lander 1	2037	MALV Cargo	$m_{i, gross}$	315.4	222.5	178.0						
			$m_{f, gross}$	243.3	178.8	132.0						
			$\Delta m_{prop}$	72.1	43.7	46.0						
Cargo Lander 2	2037	MALV Cargo	$m_{i, gross}$	230.9	156.9	124.7						
			$m_{f, gross}$	177.7	125.6	92.0						
			$\Delta m_{prop}$	53.2	31.3	32.7						
Cargo Lander 3	2037	MALV Crew	$m_{i, gross}$	287.0	200.4	160.1		390.4				
			$m_{f, gross}$	221.2	160.9	118.5		81.4				
			$\Delta m_{prop}$	65.8	39.5	41.6		309.0				
Crew Lander/ Ascent	2039	MALV Crew	$m_{i, gross}$	245.1	151.2	123.3						
			$m_{f, gross}$	173.3	124.1	90.8						
			$\Delta m_{prop}$	71.8	27.1	32.5						
Crew Transit	2039	MIST	$m_{i, gross}$	829.7	564.7		462.9		420.4	312.9	113.4	
			$m_{f, gross}$	589.8	467.3		421.0		338.7	139.4	91.4	
			$\Delta m_{prop}$	239.9	97.4		41.9		81.7	173.5	22.0	

**Table 9 Notional Campaign Major Event Mass History by Element, DAC2**

Mission	Opportunity	Vehicle Configuration	Mass Category	Event Masses, [Mg]							
				Trans-Mars Injection	Mars Orbit Insertion	Mars EDL	Mars Apotwist	Mars Ascent	Trans-Earth Injection	Deep Space Manuever	Earth Orbit Insertion
Cargo Lander 1	2037	MALV Cargo	m <sub>i, gross</sub>	304.5	234.7	188.7					
			m <sub>f, gross</sub>	234.7	188.7	139.9					
			Δm <sub>prop</sub>	69.8	46.0	48.8					
Cargo Lander 2	2037	MALV Cargo	m <sub>i, gross</sub>	219.7	168.9	135.3					
			m <sub>f, gross</sub>	168.9	135.3	99.9					
			Δm <sub>prop</sub>	50.8	33.6	35.4					
Cargo Lander 3	2037	MALV Crew	m <sub>i, gross</sub>	275.6	212.2	170.4		430.9			
			m <sub>f, gross</sub>	212.2	170.4	126.3		89.9			
			Δm <sub>prop</sub>	63.4	41.8	44.1		341.0			
Crew Lander/ Ascent	2039	MALV Crew	m <sub>i, gross</sub>	232.8	164.3	134.8					
			m <sub>f, gross</sub>	164.3	134.8	99.2					
			Δm <sub>prop</sub>	68.5	29.5	35.6					
Crew Transit	2039	MIST	m <sub>i, gross</sub>	597.8	421.9		349.2		317.2	252.5	109.7
			m <sub>f, gross</sub>	424.9	349.2		317.8		255.6	112.9	89.6
			Δm <sub>prop</sub>	172.9	72.7		31.4		61.6	139.6	20.1

**K. Mass Properties**

The resulting mass estimates for the MALV and MIST configurations of MACHETE are presented in Table 10 and Table 11, respectively. Mass growth allowance (MGA) and mass margin were allocated per ANSI/AIAA Mass Properties Control for Space Systems, resulting in a “green” MGA + mass margin grading for concepts at or before the ATP milestone. [34] The usable propellants documented in the mass summaries for the MALV and MIST are higher than what the analysis in the previous section documents. There is an inherent disconnect at each analysis cycle due the iterative nature of estimating propellant load based on vehicle inert mass, which itself is based on a previous cycles estimated propellant load. This is the primary factor contributing to the differences in maximum estimated propellant demand from Table 8 versus the usable propellant documented in Table 10 for the MALV concept. The usable propellant documented in Table 11 for the MIST concept assumes the same outer mold line as the MALV and maximizes the propellant volume within that outer mold line. After design updates introduced in DAC2, primarily a solar-based power system, the estimated propellant demand was significantly lower than the maximum propellant capacity of the design concept. This delta can be reduced by optimizing the concept through subsequent design analysis cycles or kept as design margin and additional capability.

**Table 10 DAC2 MALV Crew Configuration Mass Summary.**

MACHETE MALV	Basic Mass (kg)	MGA (%)	Predicted Mass (kg)
<b>Mass Breakdown Structure</b>			
1.0 Structures & Mechanisms	36,672	20.6%	44,245
2.0 Propulsion	11,262	19.6%	13,466
3.0 Power	554	35.1%	748
4.0 Avionics	993	14.5%	1,138
5.0 Thermal	7,337	30.7%	9,587
6.0 ECLSS	568	20.8%	686
7.0 Crew Cabin & Access	961	20.0%	1,153
<b>Dry Mass</b>	<b>58,347</b>	<b>21.7%</b>	<b>71,022</b>
10.0 Cargo			75,000
11.0 Inert Fluids			4,923
12.0 Mass Margin			8,752
<b>Inert Mass</b>			<b>159,697</b>
20.0 Useable Propellant			320,445
<b>Total Stage Gross Mass</b>			<b>480,142</b>

**Table 11 DAC2 MIST Mass Summary.**

<b>MACHETE MIST</b>	<b>Basic Mass (kg)</b>	<b>MGA (%)</b>	<b>Predicted Mass (kg)</b>
<b>Mass Breakdown Structure</b>			
<b>1.0 Structures &amp; Mechanisms</b>	<b>15,232</b>	<b>19.9%</b>	<b>18,256</b>
<b>2.0 Propulsion</b>	<b>8,597</b>	<b>19.4%</b>	<b>10,265</b>
<b>3.0 Power</b>	<b>1,994</b>	<b>26.9%</b>	<b>2,530</b>
<b>4.0 Avionics</b>	<b>763</b>	<b>15.8%</b>	<b>884</b>
<b>5.0 Thermal</b>	<b>1,789</b>	<b>31.9%</b>	<b>2,361</b>
<b>Dry Mass</b>	<b>28,374</b>	<b>20.9%</b>	<b>34,295</b>
<b>10.0 Cargo</b>			<b>55,000</b>
<b>11.0 Inert Fluids</b>			<b>7,838</b>
<b>12.0 Mass Margin</b>			<b>4,256</b>
<b>Inert Mass</b>			<b>101,390</b>
<b>20.0 Useable Propellant</b>			<b>629,224</b>
<b>Total Stage Gross Mass</b>			<b>730,614</b>

## **VI. Conclusions**

The MACHETE concept presented in this paper helps characterize as yet unexplored regions of the larger all-chemical transportation system trade space actively being studied by NASA. Specifically, the MACHETE-based architecture synthesized here was targeted at obtaining valuable knowledge regarding large, multi-function lander/ascent vehicles leveraging kiloton-class Mars surface ISRU for Mars ascent propellant acquisition. In addition to establishing a data point in the transportation system design space, this work also identified a 300,000 kg propellant production target for an enabling Mars surface ISRU system, a target which informed design and analysis efforts on the surface systems and infrastructure detailed in companion papers. [19], [20] The concepts developed and presented in these papers will continue being utilized to study alternative architecture formulations, to help NASA make informed decisions as it lays plans for the first human mission to Mars.

## **VII. Acknowledgments**

The authors would like to recognize NASA Marshall Space Flight Center Advanced Concepts Office (ACO), NASA Glenn Research Center Compass team, and David Komar of NASA Langley Research Center Vehicle Analysis Branch in the Systems Analysis and Concepts Directorate for their significant efforts crucial to the development and refinement of the concept presented in this manuscript.

## References

- [1] Portree, D. S., "Humans to Mars: Fifty Years of Mission Planning, 1950-2000", NASA Monographs in Aerospace History Series, Number 21, February 2001.
- [2] Melroy, P., "Moon to Mars Objectives", NASA Headquarters, September 2022
- [3] Drake, B. G. and Watts, K. D., "Human Exploration of Mars Design Reference Architecture 5.0", NASA/SP-2009-566, NASA Headquarters, July 2009.
- [4] Polsgrove, Tara P., Chapman, J., Sutherlin, S., Taylor, B., Fabisinski, L., Collins, T., Cianciolo, A., Samareh J., Robertson, E., Studak, W., Vitalpur, S., Lee, A., Rakow, G. "Human Mars Lander Design for NASA's Evolvable Mars Campaign," IEEE Aerospace Conference, Big Sky, MT, March 2016.
- [5] Smith, M., Bleacher, J., Craig, D., Cremens, T., Mahoney, E., Robinson, J. A., Rucker, M. "NASA's Path from Low-Earth Orbit to the Moon and on to Mars," 71st International Astronautical Congress (IAC), Virtual, October 2020.
- [6] Rucker, M. A., Craig, D. A., Burke, L. M., Chai, P. R., Chappell, M. B., Drake, B. G., Edwards, S. J., Hoffman, S., McCrea, A. C., Trent, D. J., Troutman, P. A., "NASA's Strategic Analysis Cycle 2021 (SAC21) Human Mars Architecture," 2022 IEEE Aerospace Conference (AERO), Big Sky, MT, USA, 2022.
- [7] Polsgrove, Tara P., Thomas, H. D., Dwyer Cianciolo, A., Collins, and Samareh J., "Mission and Design Sensitivities for Human Mars Landers Using Hypersonic Inflatable Aerodynamic Decelerators," IEEE Aerospace Conference, Big Sky, MT, March 2017.
- [8] Lillard, R., Olejniczak, J., Polsgrove, T., Cianciolo, A., Munk, M., Whetsel, C., Drake, B., "Human Mars EDL Pathfinder Study: Assessment of Technology Development Gaps and Mitigations," IEEE Aerospace Conference, Big Sky, MT 2017.
- [9] Samareh, J. A., Komar, D. R., Lang, C. G., Langston, S., Tartabini, P. V., Dillman, R. A., Dwyer Cianciolo, A. M. "Systems Analysis and Tradespace Exploration of Hypersonic Inflatable Entry Systems for Human Mars Mission", NASA/TM-2017-219678, NASA Headquarters, October 2017.
- [10] Polsgrove, T., Thomas, D., Sutherlin, S., Stephens, W., Rucker, M. "Mars Ascent Vehicle Design for Human Exploration," AIAA Space Forum, Pasadena, CA, August 2015.
- [11] Polsgrove, T. P., Thomas, H. D., Collins, T., Rucker, M., Zwack, M. R., Dees, P. D. "Human Mars Ascent Vehicle Configuration and Performance Sensitivities," IEEE Aerospace Conference, Big Sky, MT, March 2017
- [12] Zwack, M. R., Dees, P. D., Thomas, H. D., Polsgrove, T. P., Holt, J. B. "Program to Optimize Simulated Trajectories II (POST2) Surrogate Models for Mars Ascent Vehicle (MAV) Performance Assessment," NASA/TM-2017-219842, NASA Headquarters, December 2017.
- [13] Trent, D.J., et.al., "Updated Human Mars Ascent Vehicle Concept in Support of NASA's Strategic Analysis Cycle 2021", IEEE Aerospace Conference, Big Sky, 2022.
- [14] Tara Polsgrove, Alicia M. Dwyer-Cianciolo, Edward A. Robertson, Thomas K. Percy, Jamshid Samareh, Jay Garcia, Rafael Lugo, Ron Sostaric, Chris Cerimele and Joseph A. Garcia. "Human Mars Entry, Descent, and Landing Architecture Study: Rigid Decelerators," AIAA 2018-5192. 2018 AIAA SPACE and Astronautics Forum and Exposition. September 2018.
- [15] Ronald R. Sostaric, Christopher J. Cerimele, Edward A. Robertson and Joseph A. Garcia. "A Rigid Mid Lift-to-Drag Ratio Approach to Human Mars Entry, Descent, and Landing," AIAA 2017-1898. AIAA Guidance, Navigation, and Control Conference. January 2017.
- [16] Cichan, T. et. al., "Mars Base Camp Updates and New Concepts", Lockheed Martin Technical Paper, 2014. <https://www.lockheedmartin.com/content/dam/lockheed-martin/eo/photo/webt/Mars-Base-Camp-Update-and-New-Concepts.pdf>
- [17] Musk, E., "Making Life Multiplanetary", 68<sup>th</sup> International Astronautical Congress, Adelaide, Australia, 2017. [https://www.spacex.com/media/making\\_life\\_multiplanetary\\_transcript\\_2017.pdf](https://www.spacex.com/media/making_life_multiplanetary_transcript_2017.pdf)
- [18] Komar, D.R., Moses, R., "Hercules Single-Stage Reusable Vehicle Supporting a Safe, Affordable, and Sustainable Human Lunar & Mars Campaign", AIAA SPACE Forum, Orlando, 2017.
- [19] Olsen, S.R., et. al., "Kiloton Class ISRU Systems for LOX/LCH4 Propellant Production on the Mars Surface", AIAA SciTech Forum, Orlando, 2024
- [20] Congiardo, J.F., et. al., "Assessment of a Surface Water Transportation System Concept for ISRU Operations on Mars", AIAA SciTech Forum, Orlando, 2024
- [21] NASA, "Moon to Mars Architecture", NASA Headquarters, <https://www.nasa.gov/MoonToMarsArchitecture/>
- [22] NASA, "Moon to Mars Architecture Definition Document (ADD)", NASA Headquarters, April 2023, NASA/TP-20230002706. <https://ntrs.nasa.gov/citations/20230002706>.

- [23] Alexander, T. and Warren, E. “NASA Docking System (NDS) Interface Definitions Document”, NASA Johnson Space Center, JSC 65795 Rev. H, November 16, 2013
- [24] NASA, “Structural Design and Test Factors of Safety for Spaceflight Hardware”, NASA Headquarters, NASA-STD-5001B, October 2022, <https://standards.nasa.gov/standard/NASA/NASA-STD-5001>
- [25] Teasley, T., et. al., “Design Methodology for an Actively Cooled and Additively Manufactured GRCOP-Alloy 7,000 lbf LOX/Methane Rotating Detonation Rocket Calorimeter Chamber”, JANNAF, June 2021
- [26] Teasley, T., et. al., “Current State of NASA Continuously Rotating Detonation Cycle Engine Development”, AIAA SciTech Forum, National Harbor, 2023
- [27] Johnson, W.L., et. al., “Cryogenic Insulation Solutions for the Surface of Mars with Its Unique Environments”, Symposium on Performance, Properties and Resiliency of Thermal Insulation, June 2021.
- [28] Johnson, W.L., et. al., “Investigation into Cryogenic Tank Insulation Systems for the Mars Surface Environment”. AIAA Propulsion and Energy Forum, Cincinnati, 2018
- [29] NASA. 2015. Toughened Uni-piece Fibrous Reinforced Oxidation Resistant Composite (TUFROC). United States Patent 7,381,459 7,314,648
- [30] Falck et al., “dymos: A Python package for optimal control of multidisciplinary systems”, Journal of Open Source Software, 6(59), 2809, <https://doi.org/10.21105/joss.02809>
- [31] Edwards, S. J., and Trent, D. J., “A Model-Based Framework for Synthesis of Space Transportation Architectures” AIAA SPACE Conference, 2018. doi: 10.2514/6.2018-5133
- [32] Trent, D. J., and Edwards, S. J., “Analysis of Alternative Architectures for a 2024 Lunar Sortie” AIAA ASCEND Conference, 2020. doi: 10.2514/6.2020-4087
- [33] Goodman, J. L., Reichert, C. M., “History of Space Shuttle Rendezvous”, JSC-63400 Revision 3, October 2011, <https://ntrs.nasa.gov/citations/20110023479>
- [34] American Institute of Aeronautics and Astronautics, “Mass Properties Control for Space Systems”, ANSI/AIAA S-120A-2015, October 2015, <https://doi.org/10.2514/4.103858.001>